

## The effect of texture on the shaft surface on the sealing performance of radial lip seals

GUO Fei, JIA XiaoHong<sup>\*</sup>, GAO Zhi & WANG YuMing

*State Key Laboratory of Tribology, Tsinghua University, Beijing 100084, China*

Received September 25, 2013; accepted November 4, 2013; published online April 14, 2014

On the basis of elastohydrodynamic model, the present study numerically analyzes the effect of various microdimple texture shapes, namely, circular, square, oriented isosceles triangular, on the pumping rate and the friction torque of radial lip seals, and determines the microdimple texture shape that can produce positive pumping rate. The area ratio, depth and shape dimension of a single texture are the most important geometric parameters which influence the tribological performance. According to the selected texture shape, parameter analysis is conducted to determine the optimal combination for the above three parameters. Simultaneously, the simulated performances of radial lip seal with texture on the shaft surface are compared with those of the conventional lip seal without any texture on the shaft surface.

**rotary lip seal, elastohydrodynamics, surface texture, pumping rate, friction torque**

**PACS number(s):** 47.11.Df, 47.15.Rq, 47.55.Ca, 47.85.Dh

**Citation:** Guo F, Jia X H, Gao Z, et al. The effect of texture on the shaft surface on the sealing performance of radial lip seals. *Sci China-Phys Mech Astron*, 2014, 57: 1343–1351, doi: 10.1007/s11433-014-5404-6

Radial lip seals are widely used in the lubrication area of rotating machinery to prevent leakage and exclude contamination. A schematic of a typical installed lip seal including components is shown in Figure 1, and the sealing zone between the lip and the shaft is shown in Figure 2.

In all successful lip seals, leakage is prevented by a reverse pumping action. This reverse pumping action leads to the lubricating oil flowing from the air-side of the lip seal to the oil-side, the direction of which reverses the normal leakage flow direction from the oil-side of lip seals to the air-side. The pumping action of lip seal is considered to be principally induced by the asperities on the lip surface. When the lip seal is in use, the shear stress between the lip and shaft makes the asperities produce vane-like patterns, then resulting in axial reverse pumping flow toward the oil side by the rotating shaft. The asperities also elevate hydrodynamical pressure effect of the lubricant oil film at the

sealing zone, which can enhance the load support to maintain the film existence [1–4]. The existence of lubricant film greatly reduces the friction torque between the shaft and lip seal, which affects the wear of the sealing lip, service life and system reliability. So, the reverse pumping rate and friction torque are the two most important performance indicators of evaluating whether the radial lip seals are successful. If the reverse pumping rate is too small, the seal will produce a leak. But the reverse pumping rate must not be too high or the liquid-air meniscus, usually located near the air-side edge of the sealing zone, will be ingested into the sealing zone, and then there exists the possibility of dry friction due to asperities contact [5], which results in the considerable friction torque, thus accelerating the failure of lip seals.

However, experiments have shown that the reverse pumping action can also be produced by the shaft itself [6]. Thus the reverse pumping is a combined action that takes both the seal and the shaft into consideration. Salant and

<sup>\*</sup>Corresponding author (email: jiaxh@mail.tsinghua.edu.cn)

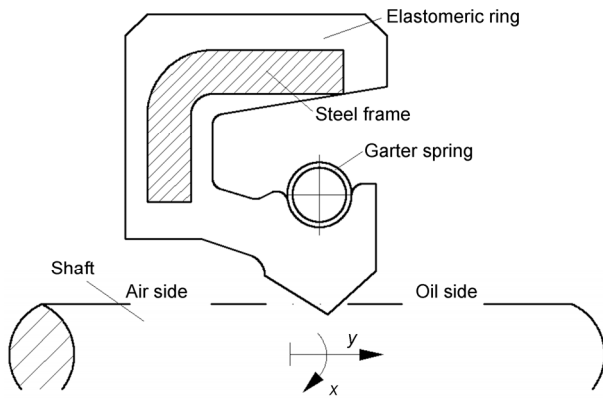


Figure 1 Cross section of radial lip seal.

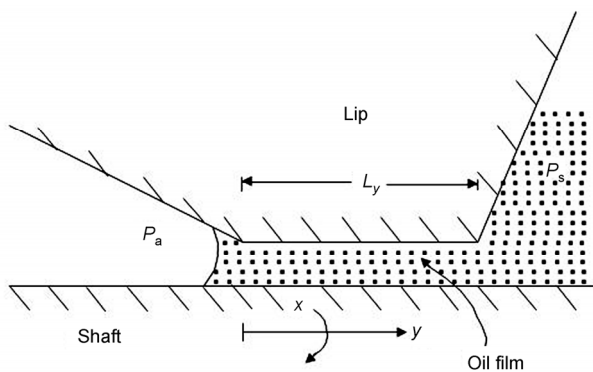


Figure 2 Schematic of the sealing zone.

Shen [7,8] have used a hydrodynamic analysis to demonstrate that even very small changes of the shaft surface asperities can create large changes in the pressure distribution within the lubricating film, resulting in producing considerable changes in the cavitation area, the load support and the reverse pumping rate. Stephens and coworkers [9–11] have used micro-electromechanical system (MEMS) manufacturing techniques to fabricate microasperities of various geometries on the shaft surface. They also demonstrate that the existence of microasperities on the shaft can enhance load capacity and decrease friction coefficient. Moreover, they have found that the oriented triangular asperities on the shaft surface produce reverse pumping rate 2.6 times greater than the conventional lip seal with natural asperities on the shaft surface. Jia et al. [12,13] have used elastohydrodynamic analysis to study the pumping rate of radial lip seals with a variety of oblique groove patterns on the shaft surfaces, which are fabricated by laser surface texturing techniques. The theoretical analysis results show good agreement with experimental results. Theoretical and experimental results show that shafts with oblique grooves can create more reverse pumping rate than the conventional lip seal containing no groove on the shaft surface.

With the rapid development of the surface processing techniques, surface texturing, as a surface modified tech-

nology, has been the focus of research interest in improving tribological performances of mechanical components. There have been many research reports and successful application cases in the mechanical seals and thrust bearings fields [14–18], the intent of which is to use different texture shapes to lower friction and wear. For radial lip seals, surface texture not only can lower friction, but also can increase reverse pumping rate, which determines sealing performance. However, it is a pity that there are very few reports besides the above mentioned in the lip seal field.

On the basis of elastohydrodynamic model established in refs. [12,13], the present study numerically analyzes the effect of various microdimple texture shapes, namely, circular, square, oriented isosceles triangular, on the pumping rate and friction torque of radial lip seals, and determines the microdimple texture shape that can produce positive pumping rate. The area ratio, depth and shape dimension of a single texture are the most important geometric parameters which influence the tribological performance. According to the selected texture shape, parameter analysis is conducted to determine the optimal combination for the above three parameters. Simultaneously, the simulated performances of radial lip seal with texture on the shaft surface are compared with those of the conventional lip seal without any texture on the shaft surface. The present study is a first step in studying the effect of texture on the shaft surface on the performances of radial lip seals by using a numerical simulation method. In the future, shaft with texture will be produced according to the simulation results of the present study, and experiments will be also conducted to validate the results.

## 1 Theoretical analysis

For the lubricant oil film thickness is much smaller than the seal radius, and the effect of curvature can be neglected, so a Cartesian coordinate system is used. The coordinate system is fixed to the shaft in order to make the research steady. The configuration schematic for the analysis is contained in Figure 3, showing two surfaces separated from a fluid film. The upper surface represents the seal lip surface, and the lower surface represents the shaft surface. The  $x$  direction represents the circumferential direction, while the  $y$  direction represents the axial direction. In order to study how the texture on shaft surface affects the sealing performances of a lip seal, it is necessary to make an assumption that the seal lip surface, i.e. the upper surface, contains no asperity.

For simplicity, the film thickness is only shown as a constant in Figure 3, although in the analysis it varies with  $x$  and  $y$ . Moreover, in order to calculate the reverse pumping rate, it is assumed that the air side of the seal is flooded with lubricant oil [19–22], as shown in Figure 2.  $L_y$  is the axial width of the sealing zone, while  $L_x$  is chosen to be the same value as  $L_y$ , representing the length of solution domain in  $x$

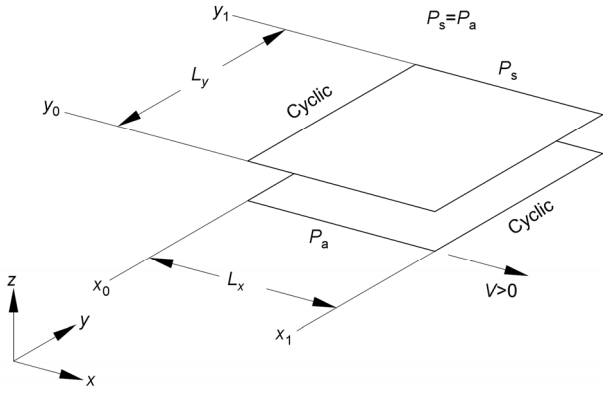


Figure 3 Boundary conditions.

direction. Thus, the analysis considers a small square section of the sealing zone that spans its axial width. The same pressure boundary condition is applied on the axial direction, representing no pressure differential in axial direction, while cyclic boundary conditions are applied on the circumferential direction. In addition, the upper surface is smooth and stationary, and the lower surface with microdimple texture shape is moving at a nonzero velocity in the  $x$  direction.

Figure 4 shows six different surfaces, corresponding to the lower surface in Figure 3, with three microdimple texture shapes, namely, circular, square, oriented isosceles triangular. The Figures 4(a) and (b) are symmetric to the center, i.e. circular and square texture shapes are omnidirectional. The orientation of isosceles triangular vertices in Figures 4(c) and (d) are parallel to the circumferential direction, while in Figures 4(e) and (f) they are parallel to the axial direction. Close attention is paid to the oriented triangular shape because it is the only geometry that is directional. As would be expected, the area ratio, depth and shape dimension of a single texture are the most important geometric parameters which influence the tribological performance of lip seals.

The area ratio  $S_p$  can be defined as:

$$S_p = \begin{cases} \frac{\pi r^2}{L_x L_y}, & \text{circular texture,} \\ \frac{ab}{L_x L_y}, & \text{square texture,} \\ \frac{ab}{2L_x L_y}, & \text{triangular texture,} \end{cases} \quad (1)$$

where  $r$  is the radius of the circular texture;  $a$  and  $b$  represent the bottom length of noncircular texture and the height of noncircular texture, respectively.

For circular texture, the shape dimension parameter  $\gamma$  represents the radius of the circle  $r$ . For square and triangular textures, it means the ratio of the height to bottom length, as presented in eq. (2):

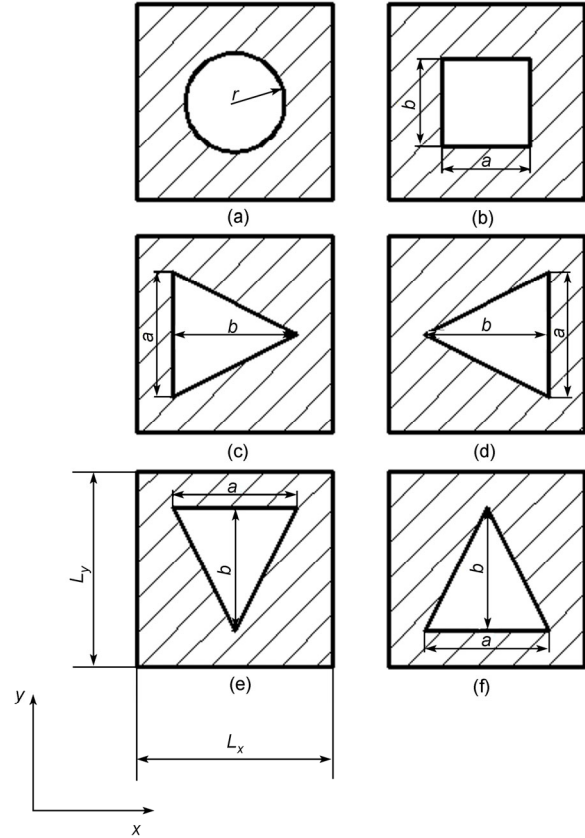


Figure 4 Microdimple texture geometries.

$$\gamma = \frac{b}{a}. \quad (2)$$

The numerical simulation model for a shaft with texture on surface operating in connection with a lip seal without any asperity consists of two coupled components: a hydrodynamic lubrication analysis of the flow at the sealing zone and a deformation analysis of the lip seal. The hydrodynamic lubrication analysis involves the solution of the Reynolds equation. As cavitation is considered, a form of the Reynolds equation that can explain cavitation is used.

$$\frac{\partial}{\partial \hat{x}} \left( H^3 \frac{\partial (F\Phi)}{\partial \hat{x}} \right) + K^2 \frac{\partial}{\partial \hat{y}} \left( H^3 \frac{\partial (F\Phi)}{\partial \hat{y}} \right) = \hat{V} \frac{\partial}{\partial \hat{x}} \{ [1 + (1-F)\Phi] H \}. \quad (3)$$

In the liquid region, non-cavitated region,

$$\Phi \geq 0, \quad F = 1 \quad \text{and} \quad P = \Phi. \quad (4)$$

In the cavitated region,

$$\Phi < 0, \quad F = 0 \quad \text{and} \quad P = 0, \quad \hat{\rho} = 1 + \Phi. \quad (5)$$

The boundary conditions are

$$\Phi = P = 0.1 \quad \text{at} \quad \hat{y} = 0 \quad (\text{air side}) \quad \text{and} \quad \hat{y} = 1 \quad (\text{liquid side}), \quad (6)$$

Cyclic boundary condition on  $\Phi$  at  $\hat{x} = 0, 1$ . (7)

In eqs. (3)–(7),  $\hat{x}$  and  $\hat{y}$  respectively represent the dimensionless circumferential coordinate and dimensionless axial coordinate;  $H$  is the dimensionless film thickness, equal to  $h/h_{\text{ref}}$ ,  $h_{\text{ref}}$  is the reference film thickness;  $F$  is the cavitation index;  $\Phi$  represents the pressure/density function defined by eqs. (2) and (3);  $K$  is the aspect ratio, equal to  $L_x/L_y$ ;  $\hat{V}$  represents the dimensionless surface speed of shaft, equal to  $6\mu L_x V / p_{\text{ref}} h_{\text{ref}}^2$ ,  $\mu$  is the viscosity of fluid,  $p_{\text{ref}}$  is the reference pressure,  $V$  is equal to  $\omega D/2$ ,  $\omega$  is the angular speed of shaft and  $D$  is the diameter of shaft;  $P$  is the dimensionless fluid pressure,  $p/p_{\text{ref}}$ ;  $\hat{\rho}$  is the dimensionless density, equal to  $\rho/\rho_0$ ,  $\rho_0$  represents fluid density.

In order to calculate the dimensionless speed  $\hat{V}$ , the viscosity needs to be known. The viscosity value is obtained from empirical formulations between the shaft speed and lubricant oil film temperature as well as between the viscosity and temperature, resulting in

$$\mu = 0.0215 \times \exp\left(-\frac{\omega}{2391.5997}\right) + 0.00399, \quad (8)$$

where  $\mu$  is in (Pa·s) and  $\omega$  is in rpm.

Eq. (1) is discretized using the finite volume method. Given the dimensionless film thickness  $H$ , the discretized form of eq. (1) is a system of linear algebraic equations, which is solved using the tri-diagonal matrix algorithm (TDMA) and relaxation iteration. A  $174 \times 174$  mesh is used, which is selected according to a mesh refinement study. When the pressure distribution is acquired, the volumetric flow rate  $Q$  is obtained from

$$Q = \int -\frac{h^3}{12\mu} \frac{\partial p}{\partial y} dx, \quad (9)$$

while the shear stress  $\tau$  on the shaft surface is obtained from eqs. (10) and (11):

$$\tau = -\frac{1}{2} h \frac{\partial p}{\partial x} + \frac{\mu V}{h} \quad (10)$$

in the liquid region, and

$$\tau = \frac{1}{2} h \frac{\partial p}{\partial x} + (1 + \Phi) \frac{\mu V}{h} \quad (11)$$

in the cavitated region. The above shear stress is used to calculate the friction torque.

The dimensional film thickness is computed by

$$h = h_s + \Delta h, \quad (12)$$

where the first term  $h_s$  represents the shaft surface structure, and the second term  $\Delta h$  represents the normal deformation of the lip.

The first term  $h_s$  is considered to be

$$h_s = \begin{cases} h_p, & \text{in texture region,} \\ 0, & \text{in non-texture region,} \end{cases} \quad (13)$$

where  $h_p$  represents the texture depth.

The second term  $\Delta h$  is calculated by the deformation analysis, which utilizes the influence coefficient method. For discretized form,

$$\Delta h_i = \sum_{k=1}^m (I)_{ik} (p_{\text{avg}} - p_{\text{sc}})_k, \quad (14)$$

where  $p_{\text{avg}}$  is the fluid pressure averaged over on cycle in the  $x$  direction.

An off-line finite element structural analysis (FEA), ANSYS, is used to calculate the influence coefficient matrix  $I$  and the static contact pressure distribution  $p_{\text{sc}}$  for the lip seal model shown in Figure 1. The effect of texture on the shaft can be ignored in the finite element analysis, for the texture depth is in several micrometers range. Solid element “plane183” is axisymmetric by default, and “target169” and “conta172” are used to define contact pair. The mesh size is 4552 elements, which is selected according to a mesh refinement study. The seal is analyzed using a Mooney-Rivlin model ( $C_{10}=1.1$  MPa,  $C_{01}=0.67$  MPa, corresponding to the elastomer material), while the shaft is treated as elastic (Young’s modulus equals 200 GPa, Poisson’s ratio equals 0.29). In obtaining influence coefficients  $(I)_{ik}$ , a unit normal force is exerted on the lip surface at the  $k$ th axial node, and the normal displacement at the  $i$ th axial node is obtained. This procedure is repeated for  $m$  times for all values of  $i$  and  $k$  from 1 to  $m$ , to generate a matrix  $I$ .

As eqs. (3)–(14) are coupled, they are solved using an iterative procedure, which is shown in Figure 5.

## 2 Results and discussion

The following parameter values are used in the present study: sealing fluid pressure  $p_s=0.1$  MPa, ambient pressure  $p_a=0.1$  MPa, cavitation pressure  $p_{\text{cav}}=0$ , diameter of the shaft  $D=100$  mm, the angular speed  $\omega=2000$  rpm. The contact width  $L_y$  is obtained from the FEA by using ANSYS.  $L_x$  is set equal to  $L_y$ , as shown in Figure 3. For each texture layout shown in Figure 4, the area ratio  $S_p$ , depth  $h_p$  and shape dimension parameter  $\gamma$  are given for analysis, as summarized in Table 1.

Figure 6 shows the local contour plot of the simulated radial stress component for a radial lip seal installed on 100 mm shaft, in the absence of the oil film. It is seen that the radial stress component decreases very rapidly away from the contact surface and its maximum occurs at the contact surface. The corresponding contact pressure  $p_{\text{sc}}$  distribution is shown in Figure 7. It is seen that the axial location of maximum pressure is closer to the liquid side of the seal

than to the air side, determining the net pumping rate, which occurs in all successful lip seals [23]. The contact width  $L_y$  is about 0.113 mm and the maximum contact pressure is about 1.04 MPa. Figure 8 shows the three dimensional plot of influence coefficient matrix  $I$ , which demonstrates that the maximum deformation occurs at the location where a load is applied.

Since lip seals are required to achieve zero leakage, an enough reverse pumping rate is firstly guaranteed, and a lowering friction torque comes secondly. Figure 9 only shows a histogram of pumping rate versus texture layout. It can be seen that the pumping rates of Nos. (a)–(d) are almost zero; the texture layout of No. (e) can produce positive pumping rate, while the texture layout of No. (f) results in negative pumping rate. The common geometrical characteristic of (a) and (b) is that these four texture shapes are sym-

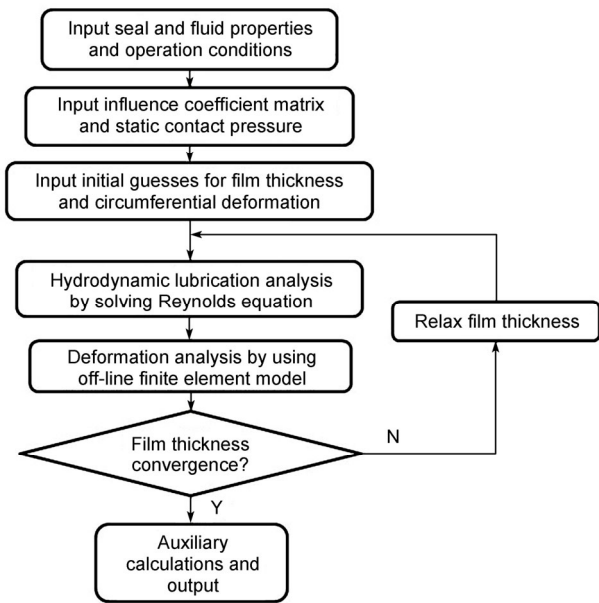


Figure 5 Computational procedure.

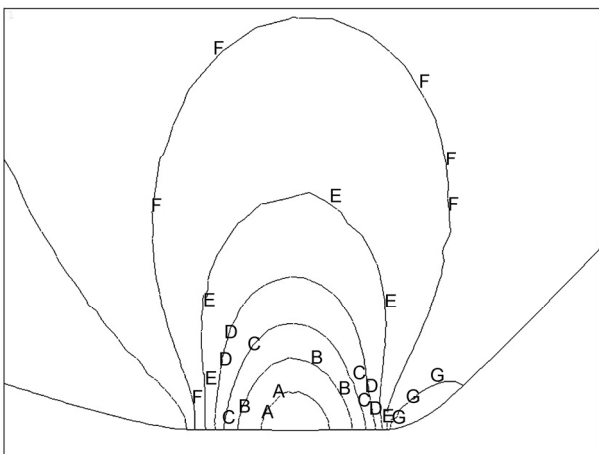


Figure 6 Local contour plot of the radial stress component at the contact zone. Stress levels: A=-1.04 MPa; B=-0.89 MPa; C=-0.74 MPa; D=-0.6 MPa; E=-0.45 MPa; F=-0.31 MPa; G=-0.16 MPa.

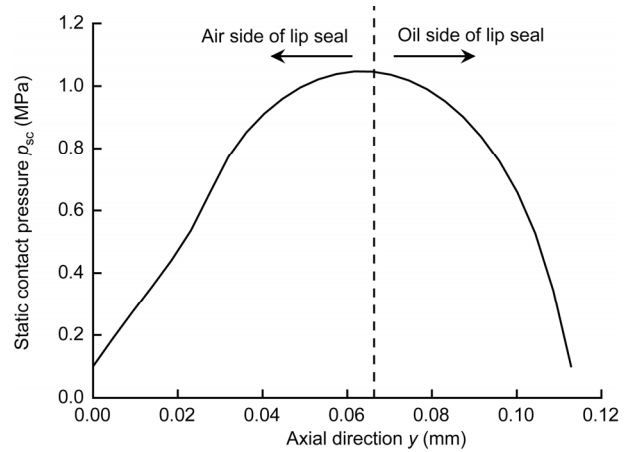


Figure 7 Static contact pressure distribution.

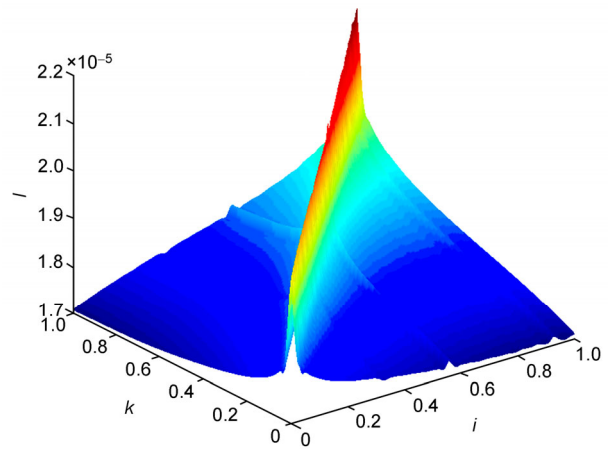


Figure 8 (Color online) Influence coefficient for radial deformations.

Table 1 Geometries parameters of surface texture

No.	Texture layout	Area ratio	Depth ( $\mu\text{m}$ )	Shape dimension
(a)		20%	3	$r$
(b)		20%	3	$\gamma=1$
(c)		20%	3	$\gamma=2$
(d)		20%	3	$\gamma=2$
(e)		20%	3	$\gamma=2$
(f)		20%	3	$\gamma=2$

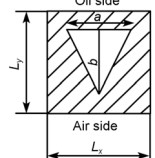
metrical in the  $x$  direction, the film distributions of which are naturally symmetrical in the  $x$  direction. As would be expected, the pressure distributions of these four texture shapes are also symmetrical in the  $x$  direction in the  $x$ - $y$  plane, shown in Figure 10. Therefore, from eq. (9), it is easy to draw the conclusion that the pumping rates of Nos. (a) and (b) must be equal to zero. So, it can be concluded that any texture that is symmetrical in the  $x$  direction has no effect on the pumping rate of a lip seal. Back to Figure 9, triangular texture on the rotating shaft, its vertex pointing to the air side, can increase pumping rate, i.e., improve sealing effect, corresponding to No. (e). The reason is that the oil pressure distribution is asymmetric to the axial direction, and the maximum pressure is close to the oil side along the axial direction, according with the reverse pumping mechanism of lip seals [24]. On the contrary, triangular texture with its vertex pointing to the oil side will increase leakage, resulting in the lip seal failure. From the above, the texture layout of No. (e) is selected to increase pumping rate, for which parameter analysis is conducted for optimal design by using the control variable method as follows.

Surface texturing, as a surface modified technology, that can improve tribological performances has been successfully applied to mechanical seals and thrust bearings fields. Many researchers suggest that the preferable area ratio of texture is 5% to 20%. So, area ratios of 10%, 15% and 20% are selected for analyzing the effect of texture on the performances of the lip seal. In order to diminish the effect of liquid flow in the texture dimple on laminar flow assumption in the Reynolds equation, 2  $\mu\text{m}$ , 3  $\mu\text{m}$  and 4  $\mu\text{m}$  are chosen as the texture depth. The shape dimension parameter of triangular texture  $\gamma$  should not be too large, or the texture will be beyond the boundaries of the contact zone in Figure 3, which may considerably affect texture effect. So, the values of  $\gamma$  are determined to be 1, 1.5 and 2. The summary of the above is shown in Table 2.

The basic data is that  $S_p$ ,  $h_p$ ,  $\gamma$  respectively equal 20%, 3  $\mu\text{m}$ , 2, in the process of parameter analysis keeping two parameters constant, and studying the other parameter how to affect the pumping rate and friction torque, according to the numerical value in Table 2. Figures 11–13 show the variations of pumping rate and friction torque with speed over different area ratios, shape dimension parameters and texture depths. It can be seen from Figure 11 that when the area ratio equals 10%, pumping rate changes a little with speed and nearly equals zero, but friction torque is very low. Although the area ratio of 10% is not suitable for lip seal system, it can be used as a reference to achieve lowering friction and wear for other kinds of seal, such as mechanical seal. For area ratio of 15%, the pumping rate increases linearly with speed, but it is smaller than that of untextured lip seal system. And the friction torque increases at first and then decreases slightly with speed. By holding all the base parameters constant except area ratio, it is easy to find that pumping rate and friction torque are both increasing with

area ratio in the range of 10%–20%, and friction torques are also smaller than that of untextured. So, area ratio of 20% is the optimum value. From Figure 12, by holding area ratio of 20% and texture depth of 3  $\mu\text{m}$  constant, pumping rates of three kinds of  $\gamma$  are all larger than that of untextured. For  $\gamma \neq 1$ , the friction torque increases with speed, and when the speed is larger than 1500 rpm, the friction torque is larger than that of untextured while the purpose of producing texture on the shaft is increasing pumping rate and simultaneously diminishing friction and wear. Obviously, the condition of  $\gamma \neq 1$  is not adopted. For  $\gamma = 1.5$ , the pumping rate increases with speed, and at 3500 rpm it suddenly increases and then precipitously decreases, which possibly results in the appearance of dry friction phenomenon, then accelerating the failure of a lip seal. Also, the condition of  $\gamma = 1.5$  is not to be adopted in lip seal system obviously. So,  $\gamma = 2$  is the optimum value. From Figure 13, when area ratio and shape dimension parameter  $\gamma$  keep constants, pumping rates of three kinds of texture depth are all increasing linearly with speed, and are all larger than that of untextured at the same speed. And, friction torques of three kinds of texture depth are all first increasing and then becoming constant with speed, and are all lower than that of untextured. Moreover, as can be seen from Figure 13, pumping rate and friction torque are both first increasing and then decreasing with texture depth in the range of 2–4  $\mu\text{m}$ . In theory, these three texture depths are all applied to shaft surface of lip seal sys-

**Table 2** Geometrical values of the selected texture layout for parameter analysis

Texture layout	Parameter	Unit	Values
	Area ratio $S_p$	%	10, 15, 20
	Depth $h_p$	$\mu\text{m}$	2, 3, 4
	Shape dimension $\gamma$	—	1, 1.5, 2

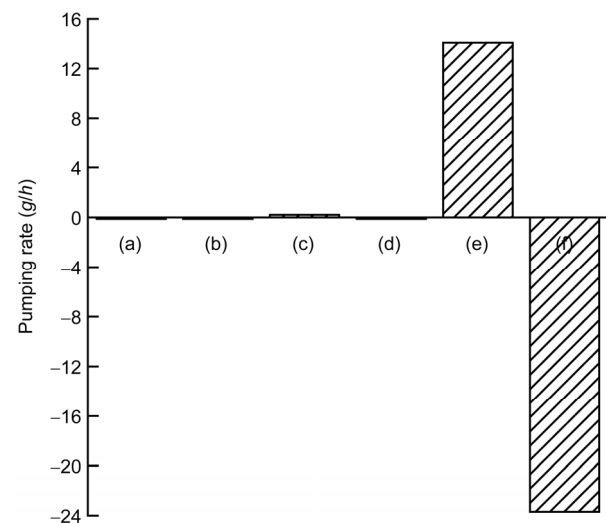


**Figure 9** Pumping rate versus texture layout.

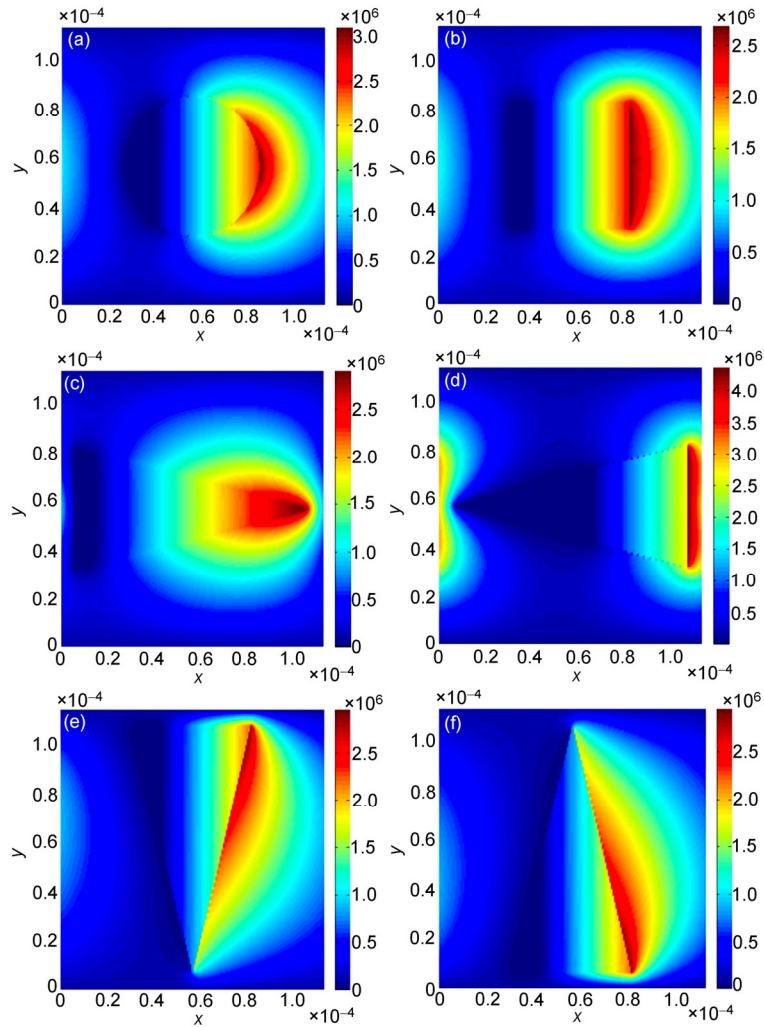


Figure 10 (Color online) Pressure distribution in the  $x$ - $y$  plane.

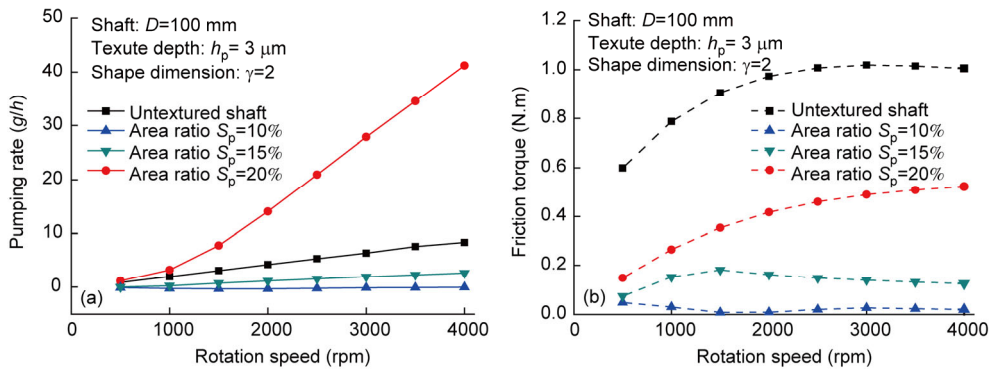
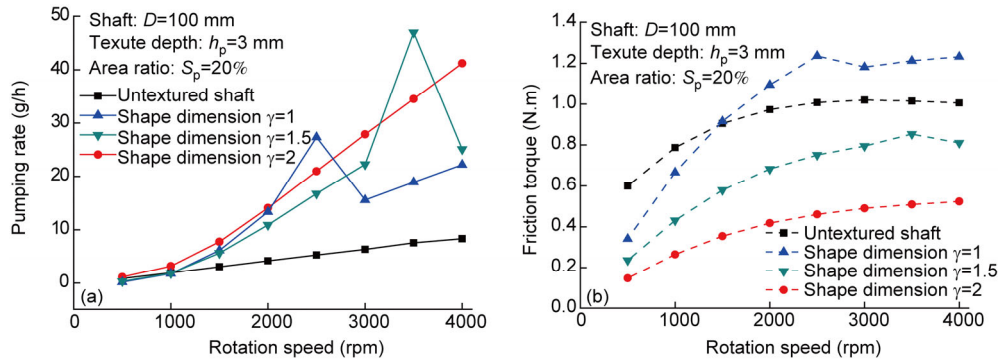


Figure 11 (Color online) (a) pumping rate and (b) friction torque versus speed at different area ratios, at the same texture depth and  $\gamma$ .

tem. However, considering the problem of manufacturing in the future, it is very difficult to manufacture the texture depth of  $2 \mu\text{m}$  by using laser processing technology. So, texture depths of  $3 \mu\text{m}$  and  $4 \mu\text{m}$  are both applicable. As the pumping rate of  $3 \mu\text{m}$  is larger, ultimately  $3 \mu\text{m}$  is selected

to be the optimum value.

In conclusion, the optimum combination of the above three parameters is that area ratio, shape dimension parameter and texture depth are respectively equal 20%, 2 and  $3 \mu\text{m}$ .



**Figure 12** (Color online) (a) pumping rate and (b) friction torque versus speed at different  $\gamma$ , at the same texture depth and area ratio.

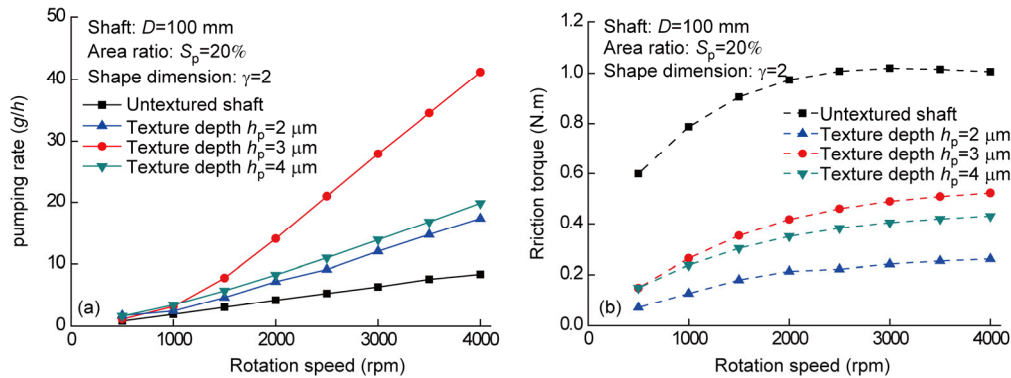


**Figure 13** (Color online) (a) pumping rate and (b) friction torque versus speed at different texture depths, at the same area ratios and  $\gamma$ .

### 3 Conclusions

On the basis of elastohydrodynamic model established in refs. [12,13], the present study numerically analyzes the effect of various microdimple texture shapes, namely, circular, square, oriented isosceles triangular, on the pumping rate and the friction torque of radial lip seals. Through analysis, the conclusion is that any texture that is symmetrical about circumferential direction has no effect on the pumping rate of a lip seal, and triangular texture on the rotating shaft, its vertex pointing to the air side, can increase pumping rate and decrease friction torque, i.e. improve sealing effect. On the contrary, triangular texture with its vertex pointing to the oil side will increase leakage, resulting in the lip seal failure.

The area ratio, depth and shape dimension parameter of a single texture are the most important geometric parameters which influence the tribological performance. According to the selected triangular texture, parameter analysis is conducted to determine the optimal combination for the above three parameters. Simultaneously, the simulated performances of radial lip seal with texture on the shaft surface are compared with those of the conventional lip seal without any texture on the shaft surface. Ultimately, the optimum combination is that area ratio, shape dimension parameter and texture depth respectively equal 20%, 2 and 3  $\mu\text{m}$ ,

which not only increase largely the pumping rate, but also decrease greatly the friction torque, compared with the conventional lip seal without any texture on the shaft surface.

The present study is the first step in studying the effect of texture on the shaft surface on the performances of radial lip seals by using a numerical simulation method. In the future, shaft with texture will be produced according to the simulation results of the present study, and experiments will be also conducted to validate the results.

*This work was supported by the National Natural Science Foundation of China (Grant No. 51175283), the National Science and Technology Major Project of China (Grant No. 2013ZX04010021) and the Specialized Research Fund for the Doctoral Program (Grant No. 20130002110006).*

- Hirano F, Ishiwata H. The lubricating condition of a lip seal. Proc Inst Mech Eng, 1965, 180: 187–196
- Jagger E T, Walker P S. Further studies on the lubrication of synthetic rubber rotary shaft seals. Proc Inst Mech Eng, 1966, 9: 191–204
- Johnston D E. Using the friction torque of rotary shaft seals to estimate the film parameters and the elastomer and the elastomer surface characteristics. In: Proceedings of the 8th BHRA International Conference on Fluid Sealing. England: British Hydromechanics Research Association Fluid Engineering, 1978. C1-1–C2-20
- Salant R F. Soft elastohydrodynamic analysis of rotary lip seals. J Mech Eng Sci, 2010, 224: 2637–2647
- Salant R F. Modeling rotary lip seals. Wear, 1997, 207: 92–99



- 6 Kunstfeld T, Haas W. Shaft surface manufacturing methods for rotary shaft seals. *Seal Technol*, 2005, 7: 5–9
- 7 Salant R F, Shen D. Hydrodynamic effects of shaft surface finish on lip seal operation. *Tribol Trans*, 2002, 45: 404–410
- 8 Shen D, Salant R F. Elastohydrodynamic analysis of the effect of shaft surface finish on rotary lip seal behavior. *Tribol Trans*, 2003, 46: 391–396
- 9 Stephens L S, Sirirpuram R, Hayden R, et al. Deterministic microasperities on bearings and seals using a modified LIGA process. *ASME J Eng Gas Turb Power*, 2004, 126: 147–154
- 10 Kortikar S N, Stephens L S, Hadinata P C, et al. Manufacturing of microasperities on thrust surfaces using ultraviolet photolithography. In: *Proceedings of the ASME Winter Topical Meeting*. Raleigh: The American Society for Precision Engineering, 2003. 148–154
- 11 Hadinata P C, Stephens L S. Soft elastohydrodynamic analysis of radial lip seals with deterministic microasperities on the shaft. *ASME J Tribol*, 2007, 129: 851–859
- 12 Jia X H, Jung S, Haas W, et al. Numerical simulation and experimental study of shaft pumping by laser structured shafts with rotary lip seal. *Tribol Int*, 2011, 44: 651–659
- 13 Jia X H, Jung S, Haas W, et al. Numerical simulation and experimental study of shaft pumping by plunge ground shafts with rotary lip seal. *Tribol Int*, 2012, 48: 155–161
- 14 Etsion I, Burstein L. A model for mechanical seals with regular microsurface structure. *Tribol Trans*, 1996, 39: 677–683
- 15 Etsion I, Kligerman Y. Analytical and experimental investigation of laser-textured mechanical seal faces. *Tribol Trans*, 1999, 42: 511–516
- 16 Etsion I. State of the art in laser surface texturing. *ASME J Tribol*, 2005, 127: 248–253
- 17 Brizmer V, Kligerman Y, Etsion I. A laser surface textured parallel thrust bearing. *Tribol Trans*, 2003, 46: 397–403
- 18 Etsion I, Halperin G, Brizmer V, et al. Experimental investigation of laser surface textured parallel thrust bearings. *Tribol Lett*, 2004, 17: 295–300
- 19 Guo F, Jia X H, Salant R F, et al. A mixed lubrication model of a rotary lip seal using flow factors. *Tribol Int*, 2013, 57: 195–201
- 20 Salant R F, Rocke A H. Hydrodynamic analysis of the flow in a rotary lip seal using flow factor. *ASME J Tribol*, 2004, 126: 156–161
- 21 Shi F H, Salant R F. Numerical study of a rotary lip seal with a quasi-random sealing surface. *ASME J Tribol*, 2001, 123: 517–524
- 22 Shi F, Salant R F. A mixed soft elastohydrodynamic lubrication model with interasperity cavitation and surface shear deformation. *ASME J Tribol*, 2000, 122: 308–316
- 23 Jia X H, Guo F, Salant R F, et al. Parameter analysis of the radial lip seal by orthogonal array method. *Tribol Int*, 2013, 64: 96–102
- 24 Müller H K, Nau B S. *Fluid Sealing Technology: Principles and Applications*. New York: Marcel Dekker Inc, 1998. 73–86